Heterogeneous Catalysis

International Edition: DOI: 10.1002/anie.201604021
German Edition: DOI: 10.1002/ange.201604021

$Cu_xCo_{1-x}O$ Nanoparticles on Graphene Oxide as A Synergistic Catalyst for High-Efficiency Hydrolysis of Ammonia–Borane

Kun Feng, Jun Zhong, Binhua Zhao, Hui Zhang, Lai Xu, Xuhui Sun,* and Shuit-Tong Lee**

Abstract: *Ammonia–borane (AB) is an excellent material for chemical storage of hydrogen. However, the practical utilization of AB for production of hydrogen is hindered by the need of expensive noble metal-based catalysts. Here, we report $Cu_xCo_{1-x}O$ nanoparticles (NPs) facilely deposited on graphene oxide (GO) as a low-cost and high-performance catalyst for the hydrolysis of AB. This hybrid catalyst exhibits an initial total turnover frequency (TOF) value of 70.0 (H_2) mol/(Cat-metal) mol·min, which is the highest TOF ever reported for noble metal-free catalysts, and a good stability keeping 94% activity after 5 cycles. Synchrotron radiation-based X-ray absorption spectroscopy (XAS) investigations suggested that the high catalytic performance could be attributed to the interfacial interaction between $Cu_xCo_{1-x}O$ NPs and GO. Moreover, the catalytic hydrolysis mechanism was studied by in situ XAS experiments for the first time, which reveal a significant water adsorption on the catalyst and clearly confirm the interaction between AB and the catalyst during hydrolysis.*

Controlled storage and release of hydrogen are well-known challenges in establishing a viable fuel-cell-based hydrogen economy.[1–3] Recently, the chemical storage of hydrogen was considered as a feasible way for practical applications.[1–8] Among the chemical hydrogen-storage materials, ammonia–borane (AB) has been regarded as a leading contender owing to its high hydrogen content (19.6 wt%), high stability in both aqueous solutions and air at room temperature, and non-toxicity.[1–9] However, until now, effective catalysts for the hydrolysis of AB are typically based on expensive and rare noble metals (such as Pt, Ru),[4,7,8] which has largely hampered applications.[3,5,7] Thus, alternate catalysts for high-efficiency hydrolysis of AB based on inexpensive non-noble metal elements are highly required and intensely studied.[3,5,7] Despite many catalysts for the hydrolysis of AB, high-performance noble metal-free catalyst with practical efficiency and sustainability remains unavailable and a daunting challenge. The catalytic mechanism regarding the electronic structure changes of the catalysts is also unclear and has largely limited the design of high-efficiency catalysts.

[*] K. Feng, Dr. J. Zhong, B. Zhao, H. Zhang, Dr. L. Xu, Prof. Dr. X. H. Sun, Prof. Dr. S. T. Lee
Institute of Functional Nano and Soft Materials Laboratory (FUNSOM), Jiangsu Key Laboratory for Carbon-Based Functional Materials & Devices, Soochow University
Suzhou 215123 (China)
E-mail: jzhong@suda.edu.cn
xhsun@suda.edu.cn
apannale@suda.edu.cn

Supporting information for this article can be found under: http://dx.doi.org/10.1002/anie.201604021.

Graphene is an outstanding supporting material for efficient catalysts, because it can enhance the catalytic performance with synergetic effects.[10–18] Recently, graphene was used to support various non-noble metal nanoparticles (NPs) for efficient catalysts for the hydrolysis of AB.[14–16] Although the hybrids showed enhanced catalytic properties, their performance remained insufficient and their electronic structure had not been well studied.[14–16] Herein we report a facile way to prepare the hybrids of $Cu_xCo_{1-x}O$ NPs on graphene oxide (GO). The optimized hybrid ($Cu_xCo_{1-x}O$-GO) shows superior catalytic performance in the hydrolysis of AB with a high initial TOF value of 70.0 (H_2) mol/(Cat-metal) mol·min. The enhanced catalytic performance of the hybrid can be ascribed to the interfacial interaction between NPs and GO. Moreover, we perform the first in situ XAS experiments to investigate the electronic structure changes of the hybrid during the hydrolysis process.

The detailed preparation and characterization of $Cu_xCo_{1-x}O$-GO samples are shown in the Supporting Information. Figure 1 shows the TEM images and elemental mappings of the $Cu_{0.8}Co_{0.2}O$-GO. Figure 1 a,b reveal that small NPs around 3 nm (Supporting Information, Figure S1) are uniformly deposited on GO. From the elemental mappings in Figure 1 c–f, Cu and Co signals can be clearly observed in the NPs, indicating the formation of Cu and Co based NPs on GO. Raman (Supporting Information, Figure S2) and XRD (Figure S3) spectra also confirm the GO feature. No new peaks in XRD pattern can be observed for the $Cu_xCo_{1-x}O$ NPs, suggesting an amorphous structure for the NPs.

The catalytic activity of various $Cu_xCo_{1-x}O$-GO samples in the hydrolysis of AB was evaluated. The TOF values are shown in the Supporting Information, Table S1. Pure GO shows no catalytic activity for the hydrolysis of AB. After decoration with various NPs, GO samples show different catalytic performance. The CoO-GO sample with only Co on GO shows practically no activity, while the CuO-GO sample with Cu on GO exhibits obvious catalytic activity with a TOF value of 9.2 (H_2) mol/(Cat-M) mol·min, suggesting Cu is an effective element for the hydrolysis of AB. Moreover, when both Co and Cu elements were deposited on GO to form bimetallic $Cu_xCo_{1-x}O$-GO samples, much higher catalytic activities compared to the single metal element-coated GO were observed, suggesting the strong synergetic effect of Co and Cu.

All $Cu_xCo_{1-x}O$-GO samples show a TOF value higher than 45.0 (H_2) mol/(Cat-M) mol·min, in sharp contrast to the value of 9.2 for CuO-GO. The TOF value increases with increasing Cu content in the bimetallic $Cu_xCo_{1-x}O$-GO samples, suggesting that Cu is the main catalytic element in

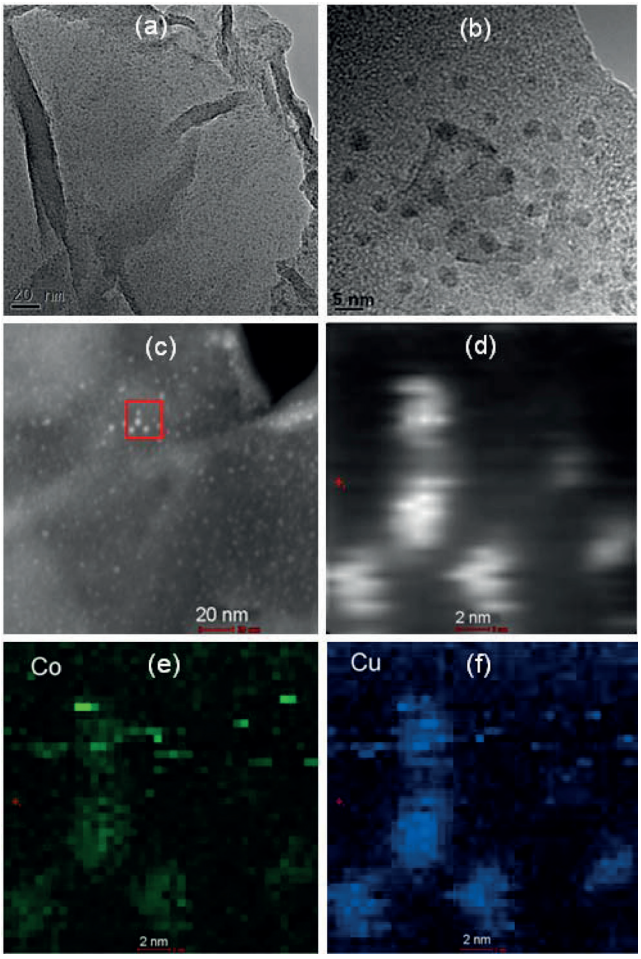

Figure 1. a) TEM and b) High-resolution TEM images of $Cu_{0.8}Co_{0.2}O$-GO. c)–f): Dark-field TEM images and the corresponding elemental mappings of $Cu_{0.8}Co_{0.2}O$-GO: Co (green) and Cu (blue) distribution in the selected area.

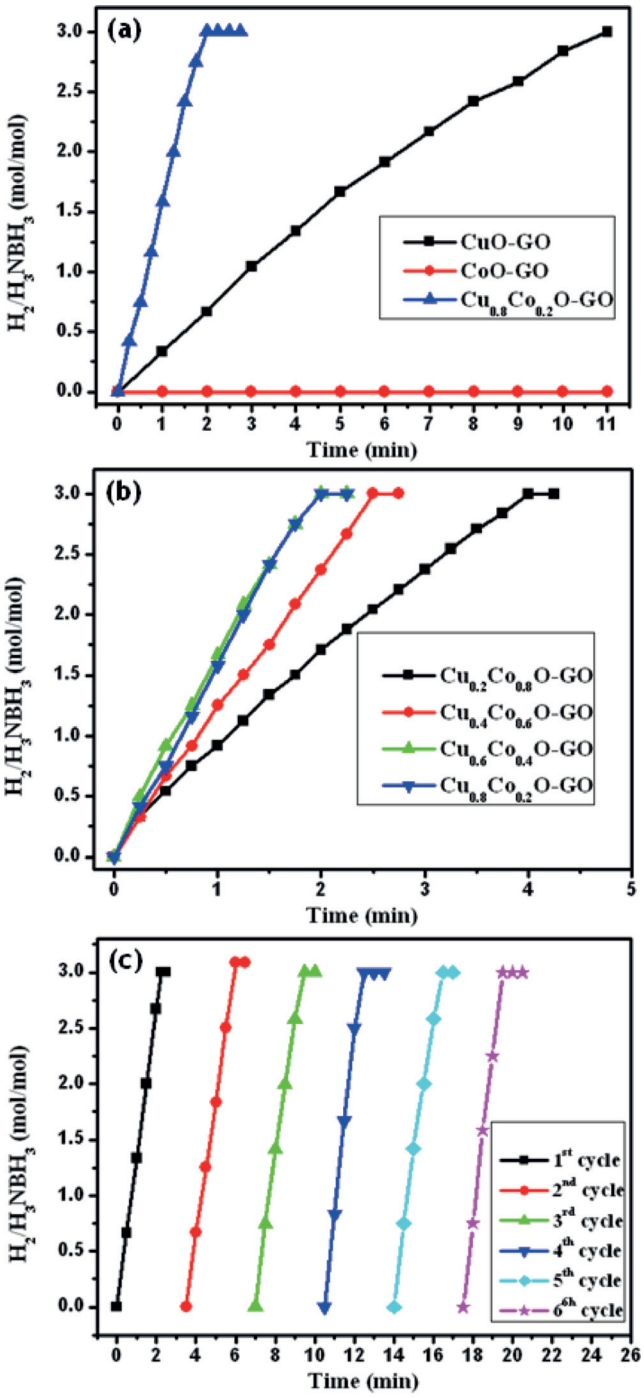

Figure 2. a) Hydrogen evolution curves of the hydrolysis of AB aqueous solution catalyzed by CuO-GO, CoO-GO, and $Cu_{0.8}Co_{0.2}O$-GO. 0.5 mmol AB was used and finally 34 mL hydrogen gas (H_2/AB = 3:1) was generated. b) Hydrogen evolution curves of the hydrolysis of AB aqueous solution catalyzed by $Cu_xCo_{1-x}O$-GO samples with different Cu:Co ratios. c) Stability test of $Cu_{0.8}Co_{0.2}O$-GO in 6 runs. The TOF value decreases from 70.0 to 66.3.

the hydrolysis process. The catalytic activity of the hybrids can be significantly enhanced by the addition of Co, suggesting an important synergetic effect. The hydrogen evolution curves are displayed in Figure 2a. It shows that $Cu_{0.8}Co_{0.2}O$-GO completes the hydrolysis process in 2 minutes and exhibits a much higher catalytic activity than CuO-GO and CoO-GO. The Cu:Co ratio was optimized to achive the best performance (Figure 2b; Supporting Information, Table S1) with $Cu_{0.8}Co_{0.2}O$-GO (Cu:Co = 8:2) at 9 wt% loading. Different metal element-based hybrids such as $Cu_xNi_{1-x}O$-GO and $Ni_xCo_{1-x}O$-GO were also investigated for comparison (Supporting Information, Figure S4), confirming the best performance of the $Cu_xCo_{1-x}O$-GO. The chemical state of the metal elements was tuned by reducing the $Cu_xNi_{1-x}O$-GO in H_2 at a high temperature, revealing that the present oxidized state was better for the hydrolysis (Supporting Information, Figure S5).

The optimized $Cu_{0.8}Co_{0.2}O$-GO shows unprecedented catalytic activity with a TOF value of 70.0 (H_2) mol/(Cat-M) mol·min in the hydrolysis of AB, which is the highest value ever reported for catalysts without noble metal elements. The excellent performance of $Cu_{0.8}Co_{0.2}O$-GO is evident by comparing its TOF value to those previously reported, as listed in the Supporting Information, Table S2. Figure 2c shows the good stability of the $Cu_{0.8}Co_{0.2}O$-GO over 6 cycles, showing that the TOF value only decreases slightly from 70.0 to 66.3 after 5 cycles (keeping 94.7% activity). The activation

energy of $Cu_{0.8}Co_{0.2}O$-GO is calculated to be 45.53 kJ mol^{-1} from the temperature-dependent curves (Supporting Information, Figure S6). The dependence of the hydrolysis reaction on $Cu_{0.8}Co_{0.2}O$-GO/AB molar ratio was also studied by keeping either the catalyst or AB amount constant at 298 K (Supporting Information, Figure S7).

We performed XAS experiments in the soft and hard X-ray ranges to study the catalytic mechanism and the synergetic effect in the $Cu_xNi_{1-x}O$-GO catalysts. The XAS spectral changes have been used to detect the interfacial interaction between Co_3O_4 nanocrystals and reduced graphene oxide, and the synergistic effect for enhanced catalytic performance.[13] Soft X-ray XAS spectra are displayed in Figure 3.

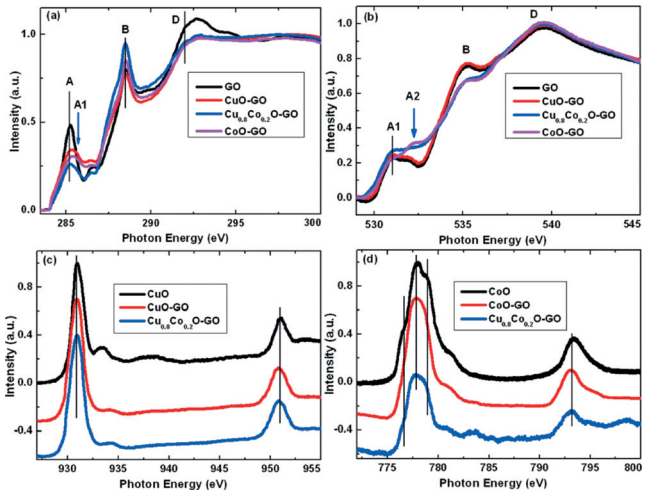

Figure 3. XAS spectra of CuO-GO, CoO-GO, and $Cu_{0.8}Co_{0.2}O$-GO at C K-edge (a),O K-edge (b), Cu L-edge (c), and Co L-edge (d). The spectra of standard samples, such as GO, CuO, and CoO, are also shown for comparison.

The C K-edge XAS spectra are shown in Figure 3a. For pure GO, three main absorption features can be observed and labeled as A, B, and D at 285.4, 288.5, and 291.7 eV, respectively. Feature A is typically assigned to the π* states of the carbon ring structure, feature D to the σ* states, and feature B to the bonding between carbon and other elements such as C=O and COOH.[13,17–20]

For pure GO, a strong feature B indicates the heavily oxidized nature of graphene. However, after NPs decoration on GO, the XAS spectra of CuO-GO and CoO-GO show an increase in feature B and a decrease in feature A. The increased feature B can be ascribed to the interfacial interaction between NPs and GO, as previously reported.[13,21] Since the external bonding with the increased feature B changes the π* orbitals of the carbon ring structure, it typically leads to a concurrently decreased feature A.[19] Further, the spectrum of CoO-GO shows a lower feature A and a higher feature B than those of CuO-GO, indicating a stronger interfacial interaction in CoO-GO. Moreover, the spectrum of the bimetallic $Cu_{0.8}Co_{0.2}O$-GO shows the highest feature B and the lowest feature A, revealing the interfacial interaction between NPs and GO is the strongest in all the samples. Cu is the main catalytic element for AB hydrolysis (Supporting Information, Table S1), while the higher feature B in the XAS spectra of CoO-GO than CuO-GO shows a stronger interfacial interaction in CoO-GO than CuO-GO, indicating Co is a more effective element for the interaction. A new feature A1 can also be observed in the spectra of the hybrid samples, but is absent in pure GO, further confirming the interfacial interaction.[17] The addition of Co in the bimetallic sample can play an important role to enhance the bonding between NPs and GO yielding a stronger synergistic effect.

Since GO has a large amount of surface functional groups, which can anchor NPs, a strong interaction between GO and NPs will form through the metal–O–C bonds, as have been detected by the XAS spectra. The interaction between metal elements and GO can form a new hybridized electronic state, different from that in the metal elements or GO alone. The hybridized state of the hybrid can help to improve the catalytic process, thus enhancing the performance of $Cu_xCo_{1-x}O$-GO in the hydrolysis of AB.

Figure 3b displays the O *K*-edge XAS spectra. The spectrum of pure GO shows the typical features for oxidized carbon and is almost identical to that of CuO-GO.[22,23] A new feature A2 at 532.5 eV is observed for both CoO-GO and $Cu_{0.8}Co_{0.2}O$-GO, which can be assigned to the Co–O bonds.[24] Figure 3c and 3d display the Cu and Co L-edge XAS spectra, respectively, revealing the oxidized state of Cu (CuO) and Co (CoO) in $Cu_{0.8}Co_{0.2}O$-GO. X-ray photoelectron spectroscopy (XPS) was also used to confirm the oxidized state of Cu and Co in the hybrids (Supporting Information, Figure S8).

We investigate the catalytic mechanism by using in situ XAS experiments to probe the electronic structure changes in the hydrolysis process. To the best of our knowledge, we present the first in situ XAS study on the hydrolysis process of AB. The experimental set up for the in situ experiments can be found in the Supporting Information, Figure S9. Considering Cu plays the main catalytic role, we focused on the XAS measurements of the Cu element.

Figure 4a shows the normalized XAS spectra of the samples at the Cu K-edge. The XAS spectrum of $Cu_{0.8}Co_{0.2}O$-GO before the hydrolysis reaction is similar to that of CuO. A Fourier transform of the extended X-ray absorption fine structure (EXAFS) data is shown in Figure 4b, in which the peak around 1.5 Å can be attributed to Cu–O bonds, while the peak around 2.5 Å to neighboring Cu-Cu configurations. The $Cu_{0.8}Co_{0.2}O$-GO shows decreased Cu-O intensity and no Cu-Cu configuration, which can be attributed to the nano size effect.

The in situ XAS spectra of $Cu_{0.8}Co_{0.2}O$-GO at Cu *K*-edge are displayed in Figure 4c. The immersion of $Cu_{0.8}Co_{0.2}O$-GO powder in pure water (without AB) yields the red curve in Figure 4c, showing significant spectral changes with a much decreased feature B and a shift of the broadened feature A to lower energy position. Typically, a decrease of feature B indicates less unoccupied orbitals, suggesting lower chemical state of Cu. The shift of feature A to lower energy position also means a reduced chemical state of Cu. Thus, after immersion in water $Cu_{0.8}Co_{0.2}O$-GO undergoes a significant chemical state change as evident from the XAS spectra,

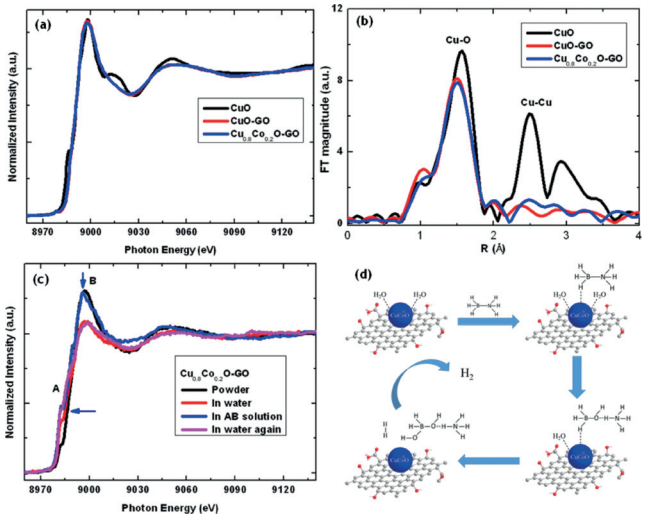

Figure 4. a) Hard X-ray XAS spectra of CuO, CuO-GO, and $Cu_{0.8}Co_{0.2}O$-GO at the Cu K-edge; b) Fourier transform of the EXAFS data; c) in situ hard X-ray XAS spectra of $Cu_{0.8}Co_{0.2}O$-GO at Cu K-edge; d) illustration of the hydrolysis process of AB aqueous solution catalyzed by $Cu_{0.8}Co_{0.2}O$-GO.

signaling a charge transfer from water to Cu in $Cu_{0.8}Co_{0.2}O$-GO. The charge transfer can be attributed to the adsorption of water molecules on the $Cu_{0.8}Co_{0.2}O$-GO catalyst. Theoretical calculations suggested that the interaction between water and the catalyst may significantly affect the hydrolysis process.[3] Here, the in situ XAS experiments of $Cu_{0.8}Co_{0.2}O$-GO in water provided a direct evidence of the adsorption of water molecules on the catalyst. Further in situ experiments were performed by the addition of AB to start the hydrolysis process. Interestingly, the XAS spectrum of $Cu_{0.8}Co_{0.2}O$-GO (the blue curve) in the presence of AB partly recovers to its initial state with an increased feature B, indicating an oxidized state of Cu. The recovered chemical state of Cu strongly indicates the interaction between $Cu_{0.8}Co_{0.2}O$-GO and AB, revealing the electronic structure evolution in the catalytic process.

During the hydrolysis process the catalyst will interact with AB, thus the B–N bonds in AB is weakened.[3,25] Then water may attack the B–N bonds for further hydrolysis reaction to release H_2.[3,25] The neighboring water molecules play an important role in the hydrolysis process. The in situ XAS experiments reveals the adsorption of water molecules on $Cu_{0.8}Co_{0.2}O$-GO before the reaction. However, once the hydrolysis starts, the AB molecules will interact with the catalyst, which may remove the adsorption of water. The adsorbed water can approach both the catalyst and AB molecule very closely, and help to attack the B–N bonds for further hydrolysis. We illustrate this process in Figure 4d. The interaction between catalyst and AB can be easily changed by removing AB from the system. In fact, when we removed the AB solution from the reaction cell and added pure water, the measured XAS spectrum in Figure 4c shows again a reduced state of Cu, revealing the electronic structure of the catalyst in water is recovered.

In summary, we report a hybrid material of $Cu_xCo_{1-x}O$ NPs on GO as a synergetic catalyst for high-performance hydrolysis of AB. The hybrid shows an initial TOF value of 70.0 (H_2) mol/(Cat-metal) mol·min, which represents the best TOF value ever reported for noble metal-free catalysts. XAS studies reveal that the enhanced catalytic performance is related to the interfacial interaction between NPs and GO. In situ XAS experiments of the hybrids are performed for the first time to investigate the electronic structure changes of the hybrid during hydrolysis.

Acknowledgements

We acknowledge the beamtime of the Shanghai Synchrotron Radiation Facility (SSRF, Beamline 08U and 14W), Beijing Synchrotron Radiation Facility (BSRF), National Synchrotron Radiation Laboratory (NSRL), and National Synchrotron Radiation Research Center (NSRRC, Beamline 20A). We thank C.H. Hong, W.S. Yan, S. Zhang, Y. Wang, Z. Jiang, and L.J. Zhang for the support of XAS experiments. We acknowledge the National Basic Research Development Program of China (2012CB825800) and the National Natural Science Foundation of China (11275137, 11179032, 91333112, U1432249). This is also a project supported by the Soochow University-Western University Centre for Synchrotron Radiation Research, Jiangsu Key Laboratory for Carbon-Based Functional Materials and Devices, Collaborative Innovation Center of Suzhou Nano Science & Technology, the Priority Academic Program Development of Jiangsu Higher Education Institutions (PAPD), and the Fund for Innovative Research Teams of Jiangsu Higher Education Institutions.

Keywords: graphene oxide · heterogeneous catalysis · hydrogen storage · hydrolysis mechanism · nanoparticles

How to cite: *Angew. Chem. Int. Ed.* **2016**, *55*, 11950–11954
Angew. Chem. **2016**, *128*, 12129–12133

[1] Q. Zhu, J. Li, Q. Xu, *J. Am. Chem. Soc.* **2013**, *135*, 10210–10213.
[2] Ö. Metin, V. Mazumder, S. Özkar, S. H. Sun, *J. Am. Chem. Soc.* **2010**, *132*, 1468–1469.
[3] C. Y. Peng, L. Kang, S. Cao, Y. Chen, Z. S. Lin, W. F. Fu, *Angew. Chem. Int. Ed.* **2015**, *54*, 15725–15729; *Angew. Chem.* **2015**, *127*, 15951–15955.
[4] W. Chen, J. Ji, X. Duan, G. Qian, P. Li, X. Zhou, D. Chen, W. Yuan, *Chem. Commun.* **2014**, *50*, 2142–2144.
[5] P. Z. Li, A. Aijaz, Q. Xu, *Angew. Chem. Int. Ed.* **2012**, *51*, 6753–6756; *Angew. Chem.* **2012**, *124*, 6857–6860.
[6] S. K. Singh, A. K. Singh, K. Aranishi, Q. Xu, *J. Am. Chem. Soc.* **2011**, *133*, 19638–19641.
[7] M. Zahmakiran, S. Özkar, *Top. Catal.* **2013**, *56*, 1171–1183.
[8] W. Y. Chen, J. Ji, X. Feng, X. Z. Duan, G. Qian, P. Li, X. G. Zhou, D. Chen, W. K. Yuan, *J. Am. Chem. Soc.* **2014**, *136*, 16736–16739.
[9] H. Yen, F. Kleitz, *J. Mater. Chem. A* **2013**, *1*, 14790–14796.
[10] H. L. Jiang, T. Akita, Q. Xu, *Chem. Commun.* **2011**, *47*, 10999–11001.
[11] Y. J. Gao, D. Ma, G. Hu, P. Zhai, X. H. Bao, B. Zhu, B. S. Zhang, D. S. Su, *Angew. Chem. Int. Ed.* **2011**, *50*, 10236–10240; *Angew. Chem.* **2011**, *123*, 10419–10423.
[12] J. L. Yang, J. J. Wang, Y. J. Tang, D. N. Wang, X. F. Li, Y. H. Hu, R. Y. Li, G. X. Liang, T. K. Sham, X. L. Sun, *Energy Environ. Sci.* **2013**, *6*, 1521–1528.

[13] Y. Y. Liang, Y. G. Li, H. L. Wang, J. G. Zhou, J. Wang, T. Regier, H. J. Dai, *Nat. Mater.* **2011**, *10*, 780 – 786.
[14] W. Q. Feng, L. Yang, N. Cao, C. Du, H. M. Dai, W. Luo, G. Z. Cheng, *Int. J. Hydrogen Energy* **2014**, *39*, 3371 – 3380.
[15] X. H. Zhou, Z. X. Chen, D. H. Yan, H. B. Lu, *J. Mater. Chem.* **2012**, *22*, 13506 – 13516.
[16] J. M. Yan, Z. L. Wang, H. L. Wang, Q. Jiang, *J. Mater. Chem.* **2012**, *22*, 10990 – 10993.
[17] H. Zhang, J. Y. Liu, G. Q. Zhao, Y. J. Gao, T. Tyliszczak, P. A. Glans, J. H. Guo, D. Ma, X. H. Sun, J. Zhong, *ACS Appl. Mater. Interfaces* **2015**, *7*, 7863 – 7868.
[18] G. Q. Zhao, J. Zhong, J. Wang, T. K. Sham, X. H. Sun, S. T. Lee, *Nanoscale* **2015**, *7*, 9715 – 9722.
[19] J. Zhong, H. Zhang, X. H. Sun, S. T. Lee, *Adv. Mater.* **2014**, *26*, 7786 – 7806.
[20] A. Kuznetsova, I. Popova, J. T. Yates, M. J. Bronikowski, C. B. Huffman, J. Liu, R. E. Smalley, H. H. Hwu, J. G. G. Chen, *J. Am. Chem. Soc.* **2001**, *123*, 10699 – 10704.
[21] J. G. Zhou, J. Wang, Y. F. Hu, T. Regier, H. L. Wang, Y. Yang, Y. Cui, H. J. Dai, *Chem. Commun.* **2013**, *49*, 1765 – 1767.
[22] E. F. Aziz, N. Ottosson, S. Eisebitt, W. Eberhardt, B. Jagoda-Cwiklik, R. Vacha, P. Jungwirth, B. Winter, *J. Phys. Chem. B* **2008**, *112*, 12567 – 12570.
[23] H. K. Jeong, H. J. Noh, J. Y. Kim, M. H. Jin, C. Y. Park, Y. H. Lee, *EPL* **2008**, *82*, 67004.
[24] J. Wang, J. Zhou, Y. F. Hu, T. Regier, *Energy Environ. Sci.* **2013**, *6*, 926 – 934.
[25] Q. Xu, M. Chandra, *J. Alloys Compd.* **2007**, *446 – 447*, 729 – 732.

Received: April 27, 2016
Published online: August 17, 2016

